

See discussions, stats, and author profiles for this publication at: <https://www.researchgate.net/publication/366290503>

Performance Study of Broadband and a Dual-Band Antenna- Array of Telecommunication Systems

Article · December 2022

DOI: 10.37649/aengs.2022.176360

CITATIONS

0

READS

9

1 author:



Prof-Takialddin Al Smadi

Jerash University

63 PUBLICATIONS 208 CITATIONS

SEE PROFILE

Some of the authors of this publication are also working on these related projects:



Brigs Academics Limited; 1st edition (January 1, 2021) [View project](#)



High-Speed Small-Purpose Parallel Hybrid Architecture of Summator for Calculation Back 3x in Eighth Coding [View project](#)



Performance Study of Broadband and a Dual-Band Antenna-Array of Telecommunication Systems

Takialddin Al Smadi

Faculty of Engineering, Jerash University, Jordan

PAPER INFO

Paper history:

Received 18/11/2022
Revised 08/12/2022
Accepted 13/12/2022

Keywords:

High Performance, Modified
Broadband Butterfly
Antenna, Broad band,
Communication Systems,
Electrodynamics System
Simulation

ABSTRACT

The antenna is a Modified Broadband Butterfly Antenna (MBBA). The technical parameters of such systems are heavily influenced by the qualities of the antenna feed devices. The aperture theory of antennas uses the representation of the radiation field of the antenna as a superposition of the fields of elementary sources, characterized by their type and amplitude-phase spatial distribution. The radiation field of an antenna of finite dimensions is a superposition of inhomogeneous spherical waves emitted by the antenna elements.

This paper is primarily the study process, Radiation models were calculated using the model of the cavity plates, Simple Green model, and the strict commercial Electromagnetic Simulator. The modified active rectangular patches with the Gann diode were combined into arrays of E and H plane. Calculated and measured results for these two active arrays the beam scanning, the possibilities have been demonstrated for both arrays. The results of an electrodynamic numerical simulation were obtained. Broadband and multiband radio systems have already found widespread practical applications by utilizing basic antenna parameters and characteristics.

© 2008 Published by University of Anbar Press All rights reserved.

1. Introduction

Performance study of Broadband and a dual-band antenna- array operation system is implemented through application of multi-band or broadband antennas and distribution system. Wideband dual-band antenna with a small profile for communications systems This work investigates the construction of a small wideband dual band antenna for aerial communication systems. A modified broadband butterfly antenna serves as the antenna. The outcomes of a numerical simulation of electrodynamic were discovered. By leveraging fundamental antenna specifications and features, broadband and multiband radio systems have already found a wide variety of practical applications. The characteristics of the antenna

feed devices have a significant impact on the technical specifications of such systems., One of the tasks of modern onboard radio electronics is to create integrated electronic systems with a combined antenna system, those working on traditional frequencies used for this radio system. Thus, the problem arises development of antennas placed on the outer surface of the aircraft and having Broadband weakly directional antennas, the radiation which considered in free space are known, but manufactured by printed technology, these antennas lose their broadband. Below for preserving broadband and directional properties are encouraged to use known in radio engineering composite materials, which allow wide limits change their electro physical

parameters: dielectric and magnetic permeability, including negative values. In such materials you can create "Forbidden zone" [1], in which there is no propagation of electromagnetic microwave waves and compared with the conductor sign of the reflection coefficient is changed to back. In addition to broadband operation, the antenna must provide acceptable energy characteristics in the and, therefore, have a fairly wide radiation pattern in this sector. As well as energy and frequency characteristics are important weight and size parameters. Therefore, a significant part of the antennas for onboard telecommunication systems are made in print. There are various designs of antennas with extended working range achieved by the use of multilayer manufacturing techniques. The easiest way to expand the working strip micro strip antennas is the implementation of printed broadband antennas, described in [2]. Expansion of the operating frequency band currently is achieved primarily by matching the emitters with the feeder path. With this complicates the design of the elements of the feeder path and the radiating system. Known broadband printed antenna operating in the 40% banding the X-range. significant increase in the thickness of the radiator due to the use of the screen to expand the operating frequency range. Ultra-wideband micro strip has similar disadvantages. Antennas made on the basis of expanding slit lines.

1.2 Related Literature

A microstrip rectangular patch antenna with various slots is proposed to reduce the resonant frequency and obtain miniaturization of the antenna. The introduction of slots into the design reduced the operating frequency from 2.4 to 1.5 GHz. The use of inset-feeding technology and the FR4 substrate increased the antenna gain [3]. Another requirement of the IoT is the transmission of big data across multiple frequency bands and bands. A multi-band antenna solves the problem when different bands are active for different frequency bands. Multiband in the design of the antenna is achieved by the introduction of slots in the overlay, the defective structure of the earth and the fractal in the antenna. The advantage of a fractal antenna is its compact size, wide frequency band, frequency

independence, and low mutual coupling [4]. In addition, the reconfigurable antenna has the advantage that it operates in a multi-band mode. proposed a reconfigurable antenna capable of tuning to an operating frequency of 2.4 GHz, 1.58 GHz and 868 MHz. The proposed antenna consisted of a round plate with a diameter of 58.8 mm, mounted on a Roger RO 5880 substrate with a thickness of 0.787 mm. Antenna reconfiguration is made possible by a digital tunable capacitor (DTC). DTC (pe64907) was activated to achieve the required capacitance and radiation efficiency of 93% [5]. Singh et al. have proposed a five-band antenna suitable for WLAN, Wi-Max and C-band applications. The antenna in operation had a fractal stripping effect and a rectangular slit geometry. The ground plane was considered defective with an inverted U-notch and two ring slots. The scheme proposes frequency reconfiguration by simultaneously turning on three PIN diodes with parasitic structures surrounded. For the ERP antenna, one low power, low insertion loss switch SP4T was included for beam control. The proposed antenna has two layers of air-gap FR4 substrate material and resonates at 2.44 GHz with a higher front-to-back ratio. Antenna with ring resonators having loops and a round overlay is also used for multi-band operation. [6]. The flexible antenna is also an option for IoT applications due to its high radiation efficiency. Authors in Ref. proposed a U-shaped and triangular emitter with two tuning plugs. The antenna had a coplanar waveguide (CPW) and a flexible substrate formed by mixing natural rubber with SiO₂. The flexibility of the substrate material had little effect on the performance of the antenna. Photo paper has also been used as a flexible substrate for ultra-wideband antenna applications [7]. A combination of flexible ceramic, Arlon 25N, and flexible polypropylene was used to design an ultra-thin flexible antenna. The fabrication of the antenna was carried out using two suitable technologies: electrotexile and injection molding. Injection printing has the limitation that the antenna cannot be completely transparent [8]. Another substrate for a flexible antenna was also considered. The acrylic sheet used makes the antenna suitable for conformal applications [9]. CPW feed was also used on a rectangular print spot on an FR4 substrate with

a compact size of 25 x 35 mm². a new corner rounding technology was used [10]. A rounded corner system has also been proposed for a CPW-powered antenna with an inverted hex configuration. The antenna had radiation, low back lobes, and low cross polarization [11]. The folded patch antenna is also a suitable choice for IoT devices. The advantage of a folded antenna is to reduce the size and keep the same frequency [12]. The antenna came in handy for use in smart museums. The transparency of the antenna became possible due to the consideration of glass as a substrate and indium-tin oxide as transparent conductors [19]. A compact three-element radiating structure with right-handed circular polarization (RHCP) has been proposed to link a low-power wide area network to space, taking advantage of the IoT. When considering FR-4 as a substrate for the antenna circuit and feeder network based on a quasi lumped quadrature coupler, the antenna had a radiation efficiency of 69% and a gain of 3.14 dBi [20]. For IoT applications has been proposed

2. Related Work for Antenna Design

Many researchers have proposed antennas for IoT applications with various aspects. The proposed antennas have different shapes of patch, ground plane, substrate material, and feeding to match the device of application. proposed a compact antenna for dual-band operation. The antenna has a rectangular microstrip patch with two slotted patches and RT Duroid 5880 as the substrate material to be operated in the frequency range of 2.39–3.15 GHz. The antenna had a gain of 5.01 dB [15]. Another compact monopole antenna consisting of a rectangular radiator with a ground plane having a rectangular slit and L-shaped stub was implemented with a size of 9.45 × 18.5 mm² [16,17,18].

3. Antenna Arrays

A modified rectangular patch antenna proposed in and [19] was used as an array construction element. The Gunn diode was built into a rectangular hole inside the patch. This modification was introduced to address issues arising from the disruption that the active item brings to the current patch

distribution. As a result of this perturbation, higher modes can be excited, contributing to higher levels of cross-polarization. As the frequency increases, the size of the active element cap becomes not negligibly small compared to the wavelength. The active element sees a distributed impedance along the housing cover and thus proper impedance matching cannot be easily achieved. By integrating an active single-port signal into a rectangular patch hole, the antenna feed-point and input impedance are better defined, resulting in improved oscillator performance. By choosing the opening position and size, you can achieve optimal loading conditions for a single active port.

The dimensions of the rectangular microstrip patch were 10.2 mm x 15.3 mm with a rectangular opening of 4 mm x 5 mm. The overlay was made on a substrate 0.54 mm thick with $\epsilon_r=2.18$. Packed 50mW Gunn Diodes (MA49106) were built into both modified rectangular pads. Converting the active impedance of the Gunn diode to the input impedance of the patch is done by placing the diode in the center of the rectangular edge of the hole, as shown in Figure 1. Both patches were excited in the TM₀₁ mode. The DC bias for the Gunn diode is provided by a high impedance microstrip line connected at the center of the patch's non-radiating edge. Frequency tuning is carried out by changing the DC bias voltage of the Gunn diode. The rectangular hole lowered the resonant frequency of the patch and reduced the quality factor of the patch resonator. The lower quality factor made it possible to obtain a wide frequency tuning range. The Gunn diode found a suitable impedance match to oscillate at a frequency slightly above the resonant frequency of the patch. This discrepancy can be attributed to the parasitic properties of the Gunn diode. However, operating at a frequency slightly off-resonance of the patch did not degrade cross-polarization levels. Changing the bias voltage has little effect on the co-polarization and cross-polarization patterns of a single active antenna [.

Two modified patches were integrated into active arrays connected in the E plane and in the H plane. To ensure mutual synchronization of the injection, the oscillation frequencies of

the active patches were controlled by changing their DC bias voltage. Both active antennas have a tuning range of about 300 MHz, but due to the manufacturing tolerances of the Gunn diode, the two tuning ranges overlap by 200 MHz. Mutual blocking of the injection was obtained mainly due to radiative coupling. Since this coupling is weak, the capture range for both arrays were about 50 MHz. When changing the DC bias voltage of one of the active pads within the capture range, the phase of the signal emitted by this pad changed from -90° to $+90^\circ$ with respect to the synchronization signal. Thus, a beam scan was obtained. The maximum achievable scanning angle is determined by the interelement spacing in the array and the phase locking range.

3.1 E plane array

The two active oscillating antennas were coupled in E plane and placed 0.63λ apart (Fig. 1). The active patch orientation in the array introduced an additional phase shift of 180° between the signals radiated by the two patches. Radiation coupling was strong enough to assure stable operation of the array. The operating frequency was 9.68 GHz. By changing the dc bias voltage of one of the active patches a symmetrical beam scanning of $\pm 20^\circ$ around broadside has been obtained. Because of the slight asymmetry of the main beam in both the steered cases, the main beam position was not determined by the direction of the maximum but rather as the point symmetrical to the beam 3 dB points. So the center of the beam is 1 dB below maximum. The measured cross-polarization levels in the whole scanning range in the main beam direction were below -20 dB. The measured EIRP of the E plane array was about 700 mW.

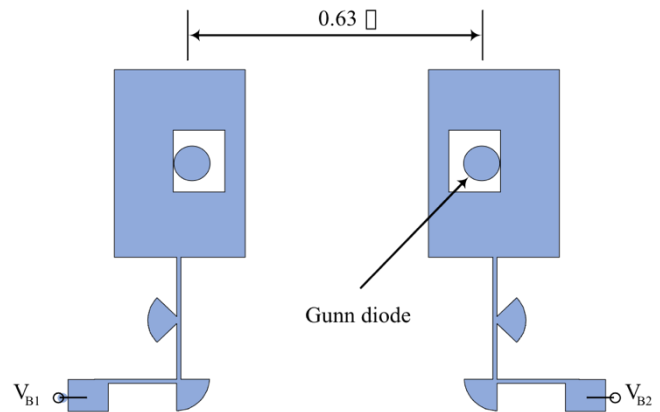


Figure 1. E Plane Active Patch Array

A combining efficiency of 109% for broadside radiation has been obtained while for the steered cases the combining efficiency is around 84%. The combining efficiency of over 100% can be explained by the fact that the Gunn diodes find better impedance matching when the active antennas are integrated in an array. In the steered cases the combining efficiency decreases because part of the power is radiated through the side lobes, which in the considered cases are quite high due to the array inter-element spacing larger than half wavelength.

3.2 Broadband waveguide

Radiators with both linear (H)-shaped and rotating polarization. The proposed design of the radiators lets in you to compose the antenna canvases with dense packing of the items in the aperture. The peculiarity of the functioning of the Antenna systems satellite tv for pc television is the paintings of the two Ku-bands with the department. This mode may be provided using one-of-a-kind schemes of production of the antenna net. right here it is viable to apply broadband factors working on two orthogonal polarizations, exhilaration that is completed with the help of broadband distribution systems, To store strength traits suitable to apply to broadband or twin emitters. The current connected, Broadband antennas, identity, navigation, and other radio structures are positioned underneath the that leads to a growth in performance and to troubles of organizing appropriate for large airplanes are located up to one hundred antennas. established on board of the antenna must have the needful directivity and does not

violate the aerodynamics and the mechanical electricity of the plane.

3.3 Broadband and dual-band micro-strip antenna

It is now widely using the antenna protruding type of cracks and printed emitters. For the formation of the shotgun Charts apply surface grid antenna of such emitters [11]. As the slot and printed antennas are the resonance, and, therefore, narrowband. One of the objectives of the modern on-board electronics is the creation of integrated electronic systems with the joint antenna system, i.e., with the antenna combined, multi frequency running on traditional used frequencies for this radio system. Thus, a task of antennas placed on the external surface of the LA and possesses a wide working range in octaves and even decades [23].

Broadband antenna, the radiation, which is seen in free space known, but manufactured on the printing technology. these antennas are losing their Broadband. Below, in order to maintain the Broadband and directed the properties of the proposed to use known in radio engineering composite materials allowing a wide range of to change their electro physical parameters.

dielectric and magnetic permeability, including negative values. In such materials, you can create a "restricted zone" [24], in which there is no distribution of electromagnetic waves of microwave and compared with the conductor of the coefficient sign reflect the changes to the return. In addition to the broadband antenna should provide an acceptable energy performance in the area of the service to users, and, therefore, have in this sector is wide enough the chart orientation. Along with the energy and frequency characteristics, the range is the weight and size parameters. Therefore, a considerable part of the antennas for airborne telecommunications systems are manufactured in the printed version, Expansion of the working micro antenna or realization of the A lot of ranged of work is usually achieved through the manufacturing of broadband antennas on the printing technology and the use of multilayer structures. An example of this is the multi-layered antenna [25,26]. However, this

antenna is not providing an opportunity to work in the Ku-band, as it has a narrower band of working on harmonization, as well as its difficult to use as an element of the antenna grid, because the pattern element is not overlapping the area of service users. For the task, you can change the structure and size of the radiation element. For example, add a loop that allows you to extend the working band. The general appearance of the micro antenna with the ring loop operating in the Ku-band (10.7 14.75 Ghz) is shown in fig. 1. Here are indicated by the following positions:

1 - The Butterfly; 2 - Coax food; 3 - loop; 4 - dielectric. For the practical implementation of the antenna substrate can be used foil dielectrics, as well as the air line. In the Fig. 2 shows the chart the direction of the aerial, shown in fig. 2, the planes of the E and N. In the Fig. 2 are identified polar in the planes of the E and H at three frequencies: 1 - 10.7 Ghz; 2 - 12.7 Ghz; 3 - 14.75 Ghz.

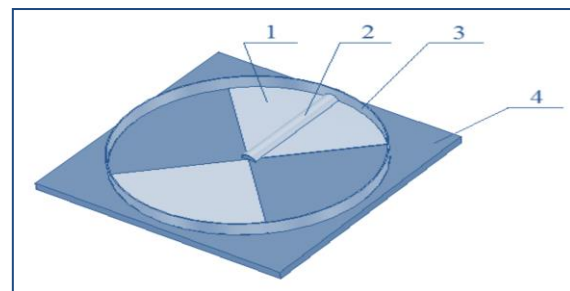


Figure 2. The general appearance of the Micro band antenna with the ring loop

The good dimension characteristics considered the antenna can be used in mobile systems. In modern mobile radio sets used the antenna with mechanical or electro-mechanical scanning. Promising direction is the development of antenna systems with electrical scanning. The sector scan in plane depends on the properties of the element; it is therefore advisable to optimize the design element in such a manner as to obtain the desired form of the chart in the local plane. For the expansion of the chart Orientation in one or two planes, you can use the periodic structure. [27,28]

4. Design Consideration of the Antenna

Modifications were made to the U-shaped reflector, either by widening or narrowing it, or by changing its shape from U-shaped to parabolic and angular.

Simulation results on the CST showed that by increasing the width of the WRA, the S11 pattern actually performs better on the LTE and GSM 900 bands, as shown in the figure. 2.

The results show that with a genuine antenna "Fig. 3" for which we keep the black coloration for the diagram, it is quite clear that the U-shaped reflector width option has a huge impact on the overall impedance and therefore affects the reflection loss. The simulation showed a slightly correct improvement in the specular image loss function in the preferred low frequency sub bands when zoomed in to 15mm. however, this slight improvement does not yet meet our goals, because the -10 dB level has not yet been implemented at these frequencies.

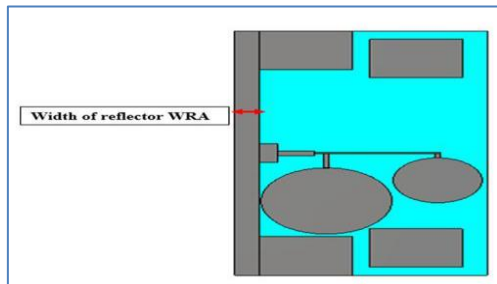


Fig 3. variant of the U-fashioned reflector width

A term specifying the frequency selectivity of the resonant circuit is the fine thing, its miles defined as the ratio between the electricity stored and the strength lost within the system. At resonance, the strength stored may be calculated both from the most magnetic subject or from the most electric powered discipline. In case of a conically depressed microstrip antenna, the overall strength stored (U_T) is defined as $U_T = U_1 + U_2 + U_3$, where U_1 is the energy due to E_z in region R_1 , U_2 is the energy due to E_z in region R_2 and U_3 is the energy due to E_ρ in region R_2 . In general the energy stored is given by,

$$U = \frac{\epsilon_0 \epsilon_{eff}}{4} \int_v |E_{max.}|^2 dv$$

Therefore,

$$U_1 = \frac{\pi E_0^2 (\frac{a}{2} - a \cot \psi)}{4\omega^2 \mu_0} (\beta_0^2 a^2 - 1) J_1^2(ka) \quad (17)$$

$$U_2 = \frac{2\pi \beta_0^2 E_0^2 \cot \psi}{4\omega^2 \mu_0} [a^2 J_2^2(ka)] \quad (18)$$

$$U_3 = \frac{2\pi \beta_0^2 E_0^2 \cot^3 \psi}{16\omega^2 \mu_0} [a^2 J_2^2(ka)] \quad (19)$$

Thus, the total radiation loss factor (Q_R) will give by :

$$Q_R = \frac{\omega U_T}{P_r} \quad (20)$$

A quality factor has been calculated for different values of plasma parameter A and half-cone angle ψ , in both the modes as shown in table (1).

5. Quality Factor

Table (1): Quality factor of a conically patch micro-strip antenna for different values of plasma parameter A and half-cone angle ψ .

A	$\psi = 90^\circ$		$\psi = 85^\circ$		$\psi = 75^\circ$	
	$Q_e \times 10^3$	$Q_p \times 10^3$	Q_e	$Q_p \times 10^3$	Q_e	$Q_p \times 10^3$
1.0	0.163	-	55.330	-	6.870	-
0.9	0.208	394.570	57.280	0.310	7.100	3.848
0.8	0.279	70.897	60.530	0.615	7.52	0.077
0.7	0.394	36.720	65.510	0.030	8.140	0.356
0.6	0.595	6.395	72.700	0.490	9.030	0.062
0.5	0.993	6.673	84.170	0.520	10.400	0.064
0.4	1.867	6.554	101.310	0.510	21.600	0.063
0.3	4.278	3.110	130.470	0.250	16.350	0.032
0.2	14.130	1.817	191.700	0.150	23.820	0.017
0.1	93.150	1.208	315.910	0.094	39.200	0.117

By adding apertures of different patterns and sizes to the circular dipole, where the pair resonance mechanism can occur, which can improve the bandwidth performance of the designed antenna. For this reason, and with this concept in mind, it is recommended to implement this approach in our matrix model to further improve bandwidth performance. The broadband and dual-band antenna assemblies and the overall performance of the antenna allow these results to be achieved with an antenna the size of a cell phone and weighing no more than 100g.

Many of these capabilities are made by various antennas used in the Wi-Fi market. Future antenna design being developed and researched requires a similar procedure to improve the electrical and mechanical properties of the designed antenna. shown in the figure 5.

The modified antenna was used to model the embedding of parasitic apertures of various bureaucracies at the front of small circular dipoles so that through inductance they could provide different resonance or even enhance the reflection coefficient over LTE and GSM bands. The square, circular, triangular or even hexagonal shapes of the apertures have been taken into account, the triangular apertures showing a satisfactory overall performance in reflectance loss expressions and features. The geometry and area of these openings are shown in Fig.6

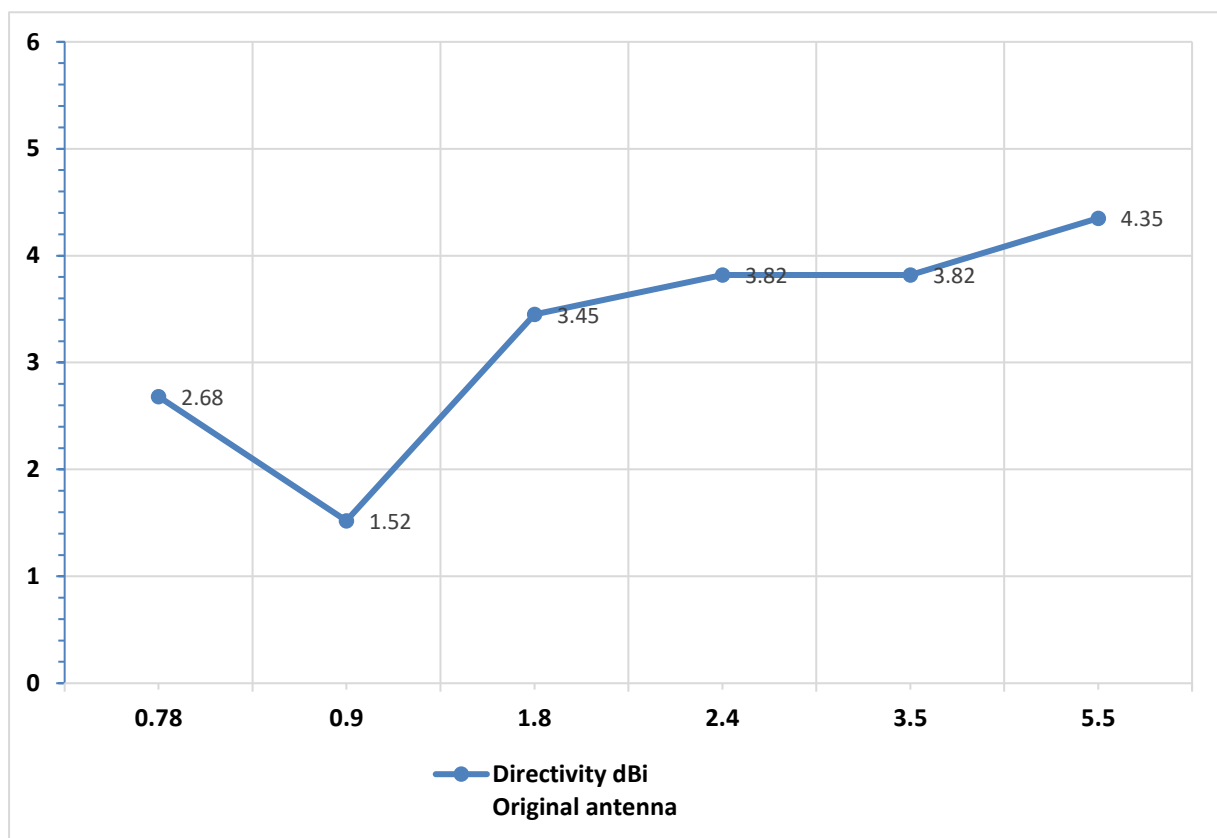


Figure 5. electric and mechanical houses of the designed antenna

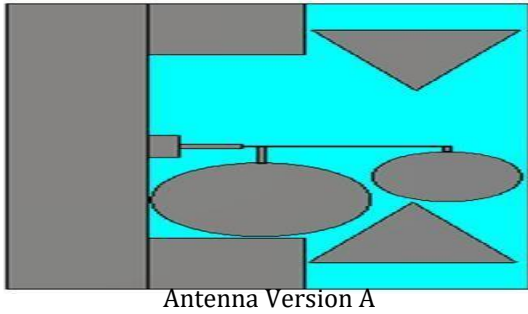


Figure 6. The proposed antenna with equilateral triangular slots.

The return loss of the array describes the extent to which the antenna matches with the input port. The lower value of the return loss enhances the performance of the antenna array. The variation of the return loss with respect to the frequency is shown in Figure 18.4. The antenna resonates at 38.6 GHz with a return loss of -33 dB. The antenna has a bandwidth of 1.3 GHz at the resonant frequency. The gain plot of the antenna at the resonant frequency is plotted and shown in Figure 7.

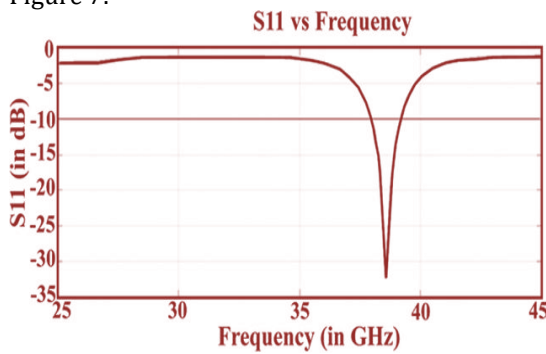


Figure 7 S11 vs frequency plot at 38.6 GHz.

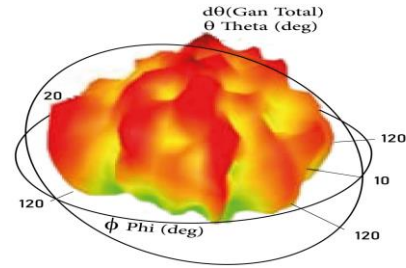


Figure 8 Gain plot at 38.6 GHz

The antenna has a gain of 10.5 dB at 38.6 GHz. The antenna exhibits a front-to-back ratio of 22 dB and a radiation efficiency of 96% at the resonating frequency. The summary of simulated results is presented in Table 2. Figure 8 represents the surface current distribution of the patch array. The flow of current in the antenna indicates good radiation.

The gain plot of the antenna at the resonant frequency is plotted and shown in Figure 9. The antenna has a gain of 10.5 dB at 38.6 GHz. The antenna exhibits a front-to-back ratio of 22 dB and a radiation efficiency of 96% at the resonating frequency.



Figure 9. Electric field distribution at 38.6 GHz

Table 2 Dimension of the antenna

L	W	a	b	c	d
3.5	5	0.6	0.1	1	2.1

Table 3 Summary of simulated results

Frequency (GHz)	S11 (< -10 dB)	Bandwidth (GHz)	Radiation efficiency (%)	Front-to-back ratio	Peak gain (dB)
38.6	-33	1.3	96	22 dB	10.5

Conclusion

The paper presents a dual band microstrip antenna containing a wide round slot. The proposed antenna is made on the FR-4 dielectric material with $\epsilon_r = 4.3$. The antenna is fed from a microstrip line with a resistance of 50 Ohm, and the optimized dimensions of the proposed antenna are $36 \times 36 \times 1.6$ mm³. A wide, circular slot is cut into the ground plane, resulting in the antenna's bandwidth doubling over the wide 1.23 and 2.4 GHz bands at 5.8 and 8.4 GHz, respectively, which fall within the C and X bands of the electromagnetic spectrum. The design provides not only a wide bandwidth, but also a significant gain at both operating frequencies. To confirm the operability of the proposed design, an antenna is manufactured and modeled. The simulation and measurement results are in good agreement. The proposed antenna array promises a promising and very redundant maximum gain of 11.5 dBi combined with a radiation efficiency of more than 83% over the entire operating range. Both one element and the entire antenna array were fabricated on a thin Rogers RT/Duroid 5880 substrate 0.254 mm thick. Antenna measurements showed a striking resemblance to the corresponding simulated effects. The antenna's small size of 40×15 mm², simple flat design, high utility, small beam width, and clean manufacturing system make it an excellent candidate for 5G communication. The proposed designs are designed for a new generation of researchers, developers and engineers.

References

- [1] Al-Sawalha, A., & Al Smadi, T. (2018). Engineering Technologies Microstrip Patch Antenna Radiation Variation of Quality Factors and Bandwidth of a Conically Depressed. *Journal of Advanced Sciences and Engineering Technologies*, 1(1), 7-10. <https://doi.org/10.32441/jaset.v1i1.53>
- [2] Hussein, A. L., Trad, E., & Al Smadi, T. (2018). Proactive algorithm dynamic mobile structure of Routing protocols of ad hoc networks. *IJCSNS*, 18(10), 86.
- [3] Al Smadi, T., & Al-Taweel, F. M. (2022). Microstrip patch Antenna Array for Wireless Design Applications. *Journal of Advanced Sciences and Engineering Technologies*, 5(1), 66-75.
- [4] Takiyaldin, A. S., Al Smadi, K., & Al-Smadi, O. O. (2017). High-Speed for Data Transmission in GSM Networks Based on Cognitive Radio. *American Journal of Engineering and Applied Sciences*, 10(1), 69-77. <https://doi.org/10.3844/ajeassp.2017.69.77>
- [5] Qian, J. F., Chen, F. C., Chu, Q. X., Xue, Q., & Lancaster, M. J. (2018). A Novel Electric and Magnetic Gap-Coupled Broadband Patch Antenna With Improved Selectivity and Its Application in MIMO System. *IEEE Transactions on Antennas and Propagation*, 66(10), 5625-5629.
- [6] Alizadeh, F., Ghobadi, C., Nourinia, J., & Mohammadi, B. (2018, May). A Novel Multi-Broadband Multi-Functional Nested Antenna For Mobile Applications. In *Electrical Engineering (ICEE), Iranian Conference on* (pp. 579-582). IEEE.
- [7] Wu P., Liu J.R., Xue Q. Wideband Excitation Technology of TE₂₀ Mode Substrate Integrated Waveguide (SIW) and Its Applications. *IEEE Trans. Microw. Theory Tech.* 2015;63:1863-1874.
- [8] Alkhalwaldeh, Igried, and Takiyaldin Al Smadi. "Micro-Strip Antenna Array for Telecommunication Systems." *European Journal of Applied Sciences-Vol 10*, no. 2 (2022).
- [9] M. N. Mohanty, S. Satrusallya, and T. Al Smadi, "Antenna selection criteria and parameters for IoT application," *Printed Antennas*, pp. 283-295, Oct. 2022, doi: 10.1201/9781003347057-18.
- [10] Ali M.T., Dzulkefli N., Abdullah R., Omar S. Design and analysis of microstrip Yagi antenna for Wi-Fi application; *Proceedings of the 2012 IEEE Asia-Pacific Conference on Applied Electromagnetics*; Melaka, Malaysia. 11-13 December 2012; pp. 283-286.
- [11] Pereira J.P.P., da Silva J.P., de Andrade H.D. A new design and analysis of a hexagonal PBG microstrip antenna. *Microw. Opt. Technol. Lett.* 2015;57:2147-2151.
- [12] Parmanand S., Swastik G. Bandwidth and gain enhancement in microstrip antenna array for 8 GHz frequency applications; *Proceedings of the 2014 Students Conference on Engineering and Systems*; Allahabad, India. 28-30 May 2014;
- [13] Takiyaldin, A. S., Al-Agha, O. I., & Alsmadi, K. A. (2018). Overview of Model Free Adaptive

- (MFA) Control Technology. *IAES International Journal of Artificial Intelligence (IJ-AI)*, 7(4), 165. <https://doi.org/10.11591/ijai.v7.i4.pp165-169>
- [14] Yang J, Wang H, Lv Z, Wang H. Design of Miniaturized Dual-Band Microstrip Antenna for WLAN Application. Kim D, Song H, Cano J-C, Wang W, Ejaz W, Du Q, eds. *Sensors (Basel, Switzerland)*. 2016;16(7):983..
- [15] Al Smadi, T., 2019. Application of Fuzzy Logic to Cognitive Wireless Communications. *Journal of advanced Sciences and Engineering Technologies*. Available at: <http://dx.doi.org/10.32441/jaset.02.01.03>
- [16] Yu Y., Hui H.T. Design of a mutual coupling compensation network for a small receiving monopole array. *IEEE Trans. Microw. Theory Tech.* 2011;59:2241–2245.
- [17] Zhu H.L., Cheung S.W., Yuk T.I. Miniaturization of patch antenna using metasurface. *Microw. Opt. Technol. Lett.* 2015;57:2050–2056.
- [18] Sharma S., Daya K.S., Sharma S., Badoo K.M., Singh M. Sol-gel auto combustion processed soft Z-type hexa nanoferrites for microwave antenna miniaturization. *Ceram. Int.* 2015;41:7109–7114.
- [19] Kundu A., Chakraborty U., Bhattacharjee A.K. Design of compact dual-band co-axially fed microstrip antenna for 2.4/5.2/5.8 GHz WLAN applications. *J. Electromagn. Waves Appl.* 2015;29:1535–1546
- [20] X. Zhang and S. Li, "Asymmetric dual-band linear-to-circular converter by bi-layered chiral metamaterial", *Int. J. RF Microw. Comput. Aided Eng.*, vol. 29, no. 10, 2019
- [21] P. Naseri, S. A. Matos, J. R. Costa, C. A. Fernandes and N. J. Fonseca, "Dual-band dual-linear-to-circular polarization converter in transmission mode application to k/ka -band satellite communications ", *IEEE Trans. Antennas Propag.*, vol. 66, no. 12, pp. 7128-7137, Dec. 2018.
- [22] M. N. Mohanty, S. Satrusallya, and T. Al Smadi, "Antenna selection criteria and parameters for IoT application," *Printed Antennas*, pp. 283–295, Oct. 2022, doi: 10.1201/9781003347057-18.
- [23] P. Naseri, F. Khosravi and P. Mousavi, "Antenna-filter-antenna-based transmit-array for circular polarization application", *IEEE Antennas Wireless Propag. Lett.*, vol. 16, pp. 1389-1392, 2016.
- [24] M. Ali Lilo, L. A. Latiff, A. bin Haji Abu, and Y. I. Al Mashhadany, "Comparison of Fault Diagnosis Approaches in Industrial Wireless Networks: A Review," *Research Journal of Applied Sciences, Engineering and Technology*, vol. 12, no. 12, 2016, doi: <https://doi.org/10.19026/rjaset.12.2876>
- [25] P. K. Malik, A. Naim, and R. Singh, "Printed Antennas," Oct. 2022, doi: 10.1201/9781003347057.
- [26] N. Barroca, H. M. Saraiva, P. T. Gouveia, J. Tavares, L. M. Borges, F. J. Velez, et al., "Antennas and circuits for ambient RF energy harvesting in wireless body area networks," in 2013 IEEE 24th annual international symposium on personal, indoor, and mobile radio communications (PIMRC), 2013, pp. 532-537.
- [27] S. Chamaani and A. Akbarpour, "Miniaturized dual-band omnidirectional antenna for body area network basestations," *IEEE Antennas Wireless Propagation Letters*, vol. 14, pp. 1722-1725, 2015.
- [28] D. Gaetano, P. McEvoy, M. J. Ammann, M. John, C. Brannigan, L. Keating, et al., "Insole antenna for on-body telemetry," *IEEE Transactions on Antennas Propagation*, vol. 63, pp. 3354-3361, 2015.
- [29] X.-Q. Zhu, Y.-X. Guo, and W. Wu, "A compact dual-band antenna for wireless body-area network applications," *IEEE Antennas Wireless Propagation Letters*, vol. 15, pp. 98-101, 2015.
- [30] P. Soontornpipit, "A dual-band compact microstrip patch antenna for 403.5 MHz and 2.45 GHz on-body communications," *Procedia Computer Science*, vol. 86, pp. 232-235, 2016.